Rare Metal Materials and Engineering
Volume 49, Issue 8, August 2020
Available online at www.rmme.ac.cn

Science Press

Cite this article as: Rare Metal Materials and Engineering, 2020, 49(8): 2607-2614.

ARTICLE

Effects of Ge Addition on the Microstructure and Thermal Stability of Co-V-Si High-Temperature Shape Memory Alloys

Wang Cuiping[1], Huang Lusheng[1], Zhang Yanqing[1], Zhang Jinbin[1], Jiang Hengxing[1], Yang Shuiyuan[1], Liu Xingjun[1,2,3]

[1] Fujian Provincial Key Laboratory of Materials Genome, Xiamen University, Xiamen 361005, China; [2] State Key Laboratory of Advanced Welding and Joining, Harbin Institute of Technology, Harbin 150001, China; [3] Institute of Materials Genome and Big Data, Harbin Institute of Technology, Shenzhen 518055, China

Abstract: A study of the Ge substitution for Si in the $Co_{64}V_{16}Si_{20}$ shape memory alloy was performed in this work. The microstructure, martensitic transformation, thermal cycle stability, and microstructural evolution during thermal cycling of the $Co_{64}V_{16}Si_{20-x}Ge_x$ (x=2, 4, 6, 8, at%) alloys were studied. When x=2, the alloy was single $D0_{22}$ martensite. With increasing Ge content to 4 at% and 6 at%, two-phase microstructure of (αCo)+$D0_{22}$ martensite was observed. When Ge content was up to 8 at%, three-phase microstructure of (αCo)+$D0_{22}$ martensite+R phase was observed. The results show that the reversible martensitic transformation temperatures increase by nearly 50 °C through adding Ge compared with that of the $Co_{64}V_{16}Si_{20}$ matrix alloy. Although the (αCo) or R phases precipitate during thermal cycling process, the reversible martensitic transformation peaks are observed during ten times thermal cycles. It reveals that the Ge addition can improve thermal cycling stability of Co-V-Si high-temperature shape memory alloy.

Key words: Co-V-Si-Ge; martensitic transformation; thermal stability; high-temperature shape memory alloys

High-temperature shape memory alloys (HTSMAs), with the martensitic transformation temperature higher than 100 °C, have drawn significant attention and interest in recent years[1,2]. To date, many HTSMA systems have been widely investigated including Ni-Ti-base[3-6], Ni-Mn-Ga-base[7-10] and Cu-Al-base[11-13], etc. Co-based alloys have received some attention in high-temperature alloys, because of their unique properties: extremely high strength, high Curie temperature and excellent corrosion resistance[14,15]. Recently, more Co-based alloys, such as Co-Cr-Ga-Si[16,17], Co-Cr-Al-Si[18], Co-V-Si(-Ga)[19,20], and Co-V-Ga[21], have been reported to exhibit high-temperature martensitic transformation.

Thermal stability has been achieved for several NiTi-base HTSMA material systems[3,6]. However, these alloys have significantly lower martensitic transformation temperature, which provides motivation for studying Co-V-Si HTSMAs. Jiang et al found an off-stoichiometric Co_2VSi Heusler-typed HTSMA[20]. The start temperatures of forward and reverse martensitic transformation (M_s and A_s) are 683 and 693 °C, respectively, higher than those of most known Heusler-type HTSMAs, but their thermal stability still needs to be improved. The effects of alloying Ga on Co_2VSi alloy has been experimentally investigated[19]. The results showed that with the increase of Ga content, the martensitic transformation temperature decreased and R phase precipitated from martensite. Also, the thermal process occurred along with (εCo) forming. In addition, the mechanical properties of the matrix alloy deteriorated with the addition of element Ga. Progress can be expected by further study on this system with specific attention to phase stability.

From the previous reports, Yu et al[22-24] replaced Ni, Fe and Ga element with Ge in the Ni-Fe-Ga alloy system. With the

Received date: August 25, 2019
Foundation item: National Natural Science Foundation of China (51571168); National Key R&D Program of China (2017YFB0702901)
Corresponding author: Liu Xingjun, Ph. D., Professor, Department of Materials Science and Engineering, College of Materials, Xiamen University, Xiamen 361005, P. R. China, Tel: 0086-592-2187888, E-mail: lxj@xmu.edu.cn

increase of Ge content, the phase transition temperature decreased linearly from 100 °C to −90 °C. The alloying of Ge improved the compression and ductility in Ni-Fe-Ga alloy. Han et al[25] using Ge instead of Sn in $Ni_{43}Mn_{46}Sn_{11}$ shape memory alloy found that the martensitic transformation temperature rose up rapidly. Lu et al[26] using Ge instead of Ga in Ni_2MnGa alloy found that the addition of Ge can reduce the martensitic transformation temperature. Xuan et al[27] studying the alloys of $Mn_2Ni_{1.6}Sn_{0.4-x}Ge_x$ (x=0.02, 0.04, 0.06, 0.08, 0.10) found that the temperature of martensite phase transition can be greatly increased by adding Ge. In the present study, the formation elements of Heusler-type structure ($L2_1$, Co_2VZ) are considered. Ge element and Si element are in the same main group (ⅣA), so the chemical property of Ge is similar to that of Si, for example they are completely miscible. Therefore, Ge is chosen as an alloying element to substitute Si partially.

This work investigated the microstructure, martensitic transformation, microstructural evolution and thermal stability of Co-V-Si-Ge alloys during thermal cycling.

1 Experiment

Using the high purity cobalt (99.9%), vanadium (99.7%), silicon (99.999%) and germanium (99.999%), polycrystalline buttons $Co_{64}V_{16}Si_{20-x}Ge_x$ (x=2, 4, 6, 8, denoted as Ge2, Ge4, Ge6, Ge8, respectively) alloys were prepared by arc melting in argon atmosphere. The ingots, around 30 g, were melted at least 5 times in order to achieve the homogeneity. Each ingot was cut into plate-shaped specimens by wire-cutting prior to heat treatment. Then, the vacuum in the quartz capsules containing the plate-shaped specimens was pumped to 5 Pa, and was backfilled with argon to 7×10^4 Pa. The above processes were repeated four times to avoid oxidation of samples. Afterwards, the samples were annealed at 1100 °C for 6 h followed by quenching into ice water.

The microstructure observation and the composition measurements of the phases were carried out using electron probe microanalysis (EPMA, JXA-8100, JEOL, Japan), when the accelerating voltage and probe currents were 20 kV and 1.0×10^{-8} A, respectively. Also mapping analysis was performed by EPMA with the accelerating voltage and probe currents of 20 kV and 3.0×10^{-8} A, respectively. Wavelength dispersive spectrometer (WDS) was used to determine the composition of the phases. The composition was determined by the mean value over five points calibrated by ZAF (Z: atomic number effect, A: absorption effect, F: fluorescence effect) correction, where pure elements were used as standard samples. After metallographic preparation, the microstructure of the alloys was investigated by optical microscope (OM) after the samples were polished and etched with the solution of 10 g $FeCl_3\cdot6H_2O$+25 mL HCl+75 mL water. The XRD measurements were carried out using Cu-Kα radiation at 40 kV and 40 mA. The data were collected in the range of 2θ from 20° to 90° at a step size of 0.0167°. Phase transformation temperatures were studied using a differential scanning calorimeter (DSC) with the heating and cooling rates of 10 °C·min^{-1} in nitrogen atmosphere.

2 Results and Discussion

2.1 Microstructure

Back scattered-electron (BSE) and optical microscope (OM) images of $Co_{64}V_{16}Si_{20-x}Ge_x$ (x=2, 4, 6, 8) alloys annealed at 1100 °C for 6 h are presented in Fig.1, and the XRD results are presented in Fig.2. A typical lamellar single martensite (M) was observed in Ge2 alloy. With the increase of Ge content, the second phase (αCo) precipitated from the grain boundaries, wherein the two-phase microstructure was observed in Ge4 and Ge6 alloys. With the substitution of Si with Ge increasing to 8 at%, the third phase (R phase) was found. The R phase

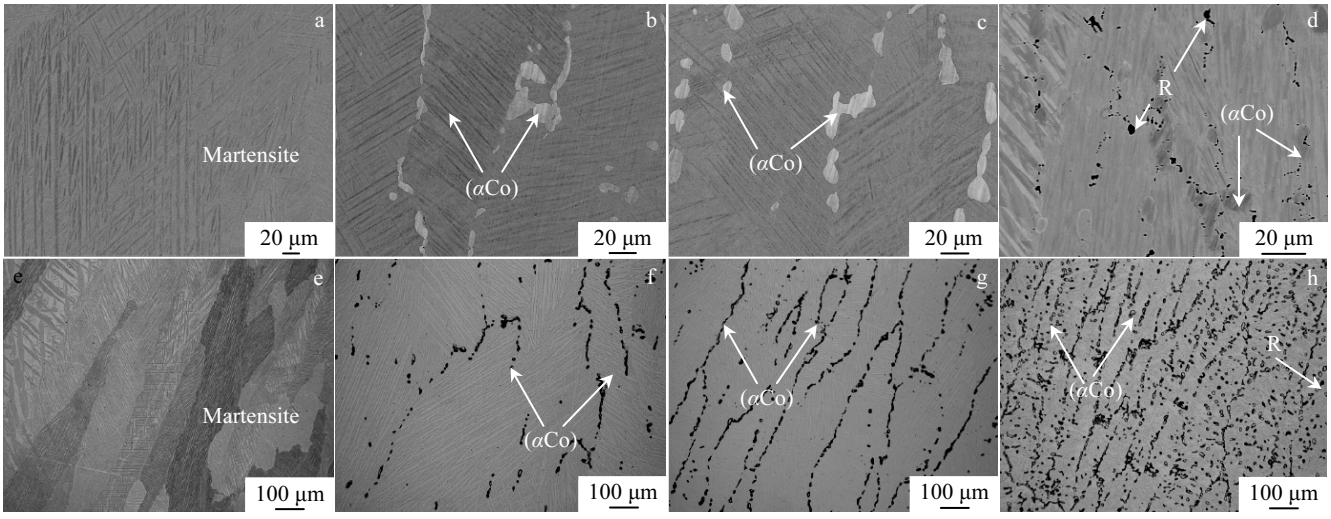

Fig.1 BSE (a~d) and OM (e~h) images of $Co_{64}V_{16}Si_{20-x}Ge_x$ alloys: (a, e) x=2, (b, f) x=4, (c, g) x=6, and (d, h) x=8

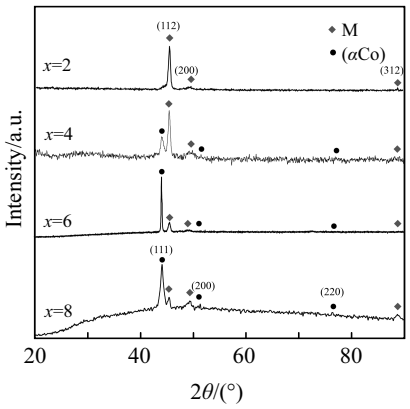

Fig.2 XRD patterns of the $Co_{64}V_{16}Si_{20-x}Ge_x$ (x=2, 4, 6, 8) alloys

($Co_{35}V_{46}Si_{19}$) in these alloys is an intermetallic compound, which was defined in the phase diagram of the Co-V-Si system reported by Gupta et al[28]. Based on the results in Ref. [19, 28], the third phase was determined to be R phase ($Co_{35}V_{46}Si_{19}$). The composition of each phase in the studied alloys is shown in Table 1.

To obtain the crystallographic information of each phase in the studied alloys, the XRD tests were carried out at room temperature and the results are shown in Fig.2. A single $D0_{22}$ martensite structure is observed in the Ge2 alloy, and the peaks are indexed to be consistent with $D0_{22}$ structure[15]. It can also be seen from Fig.2 that (αCo) phase exists in Ge4, Ge6 and Ge8 alloys. Due to the little size of (αCo) phase and distributing along the grain boundary, the diffraction peaks of the (αCo) phase are weak. However, combined with the composition analysis in Table 1, it can be basically determined that the precipitate phase is (αCo) phase. Three-phase are observed for the Ge8 alloy in Fig.1, but the diffraction peaks of the R phase are absent in Fig.2. It results from the little size and amount of R phase. When the heat treatment time is up to 3 d at 1100 °C, BSE image and X-ray diffraction patterns of the Ge8 are shown in Fig.3, and the composition mapping analysis of elements are given in Fig.4.

Table 1 Original composition of each phase in the studied alloys (at%)

Alloy	Martensite			(αCo) phase			R phase		
	V	Si	Ge	V	Si	Ge	V	Si	Ge
Ge2-1100 °C-6 h	16.12	17.93	1.90	-	-	-	-	-	-
Ge4-1100 °C-6 h	16.30	15.65	3.23	13.64	8.65	2.63	-	-	-
Ge6-1100 °C-6 h	16.05	13.64	4.91	13.63	7.41	3.79	-	-	-
Ge8-1100 °C-6 h	16.68	11.86	6.95	13.95	6.21	5.17	47.63	13.18	2.54
Ge8-1100 °C-3 d	16.98	11.52	6.97	13.80	6.30	5.20	47.14	13.30	2.59

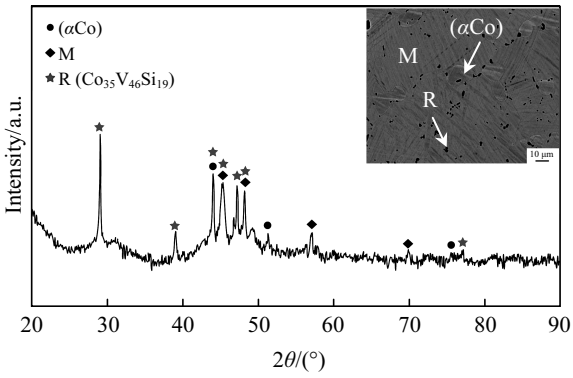

Fig.3 BSE image and XRD pattern of Ge8 alloy after annealing at 1100 °C for 3 d

2.2 Martensitic transformation behaviors

Fig.5 presents the DSC curves of the $Co_{64}V_{16}Si_{20-x}Ge_x$ (x=2, 4, 6, 8) alloys with a heating and cooling rate of 10 °C·min^{-1}. The results show that the reversible martensitic transformation peaks were observed in the forward and reverse martensitic transformation, whereas the reverse martensitic transformation of the Co-V-Si matrix alloy was absent[18]. The start (M_s and A_s) and finish (M_f and A_f) temperatures of forward and reverse martensitic transformation were obtained from the DSC curves of the $Co_{64}V_{16}Si_{20-x}Ge_x$ (x=2, 4, 6, 8) alloys and given in Table 2. The transformation thermal hysteresis was calculated using the formula: A_f−M_s. It shows that the transformation temperatures of the alloys remarkably increase with Ge alloying. For example, in the Ge2 alloy, the A_s temperature differs by about 50 °C from that of matrix alloy. There is the second endothermic peak labeled by the black arrow in DSC curves of the Ge8 alloy. It results from the precipitation of the R phase. This phenomenon will be further researched in chapter 2.3. In $Co_{64}V_{16}Si_{20}$ alloy, it is difficult to define reverse martensitic transformation finishing temperature (A_f) in the DSC curve because of the signal of $L2_1$ to A12. What's more, it is necessary to mention that in the subsequent 2nd DSC process for this sample, martensitic transformation can hardly be detected, as further improvement for thermal stability of this martensite is still needed[20]. It is worthy noting that with the Ge doping, no exothermic signal exists at the end of broad endothermic peak, indicating that the precipitation of A12 phase is suppressed during heating comparing to the $Co_{64}V_{16}Si_{20}$ matrix alloy. Thus the Ge addition can improve $L2_1$ phase stability at high temperature, implying a good thermal cycling stability.

2.3 Thermal cycling stability and microstructural evolution

DSC samples were subjected to ten times thermal cycles between room temperature and 900 °C, in order to investigate

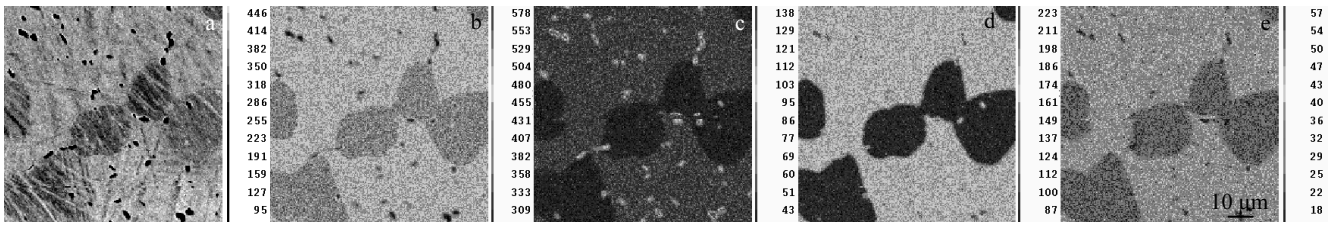

Fig.4 EPMA image (a) and composition mapping analysis of Ge8 alloy after annealing at 1100 °C for 3 d: (b) Co, (c) V, (d) Si, and (e) Ge

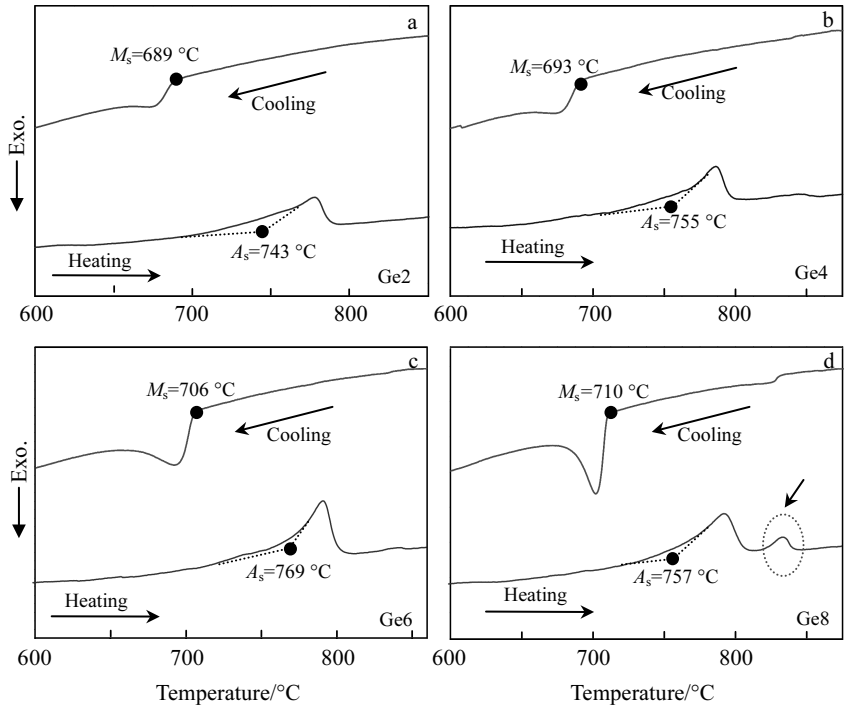

Fig.5 DSC curves of the $Co_{64}V_{16}Si_{20-x}Ge_x$ (x=2, 4, 6, 8) alloys with the heating and cooling rate of 10 °C·min^{-1}

Table 2 Martensitic transformation temperatures of the studies alloys (°C)

Alloy	A_s	A_f	M_s	M_f	Hysteresis
Ge0[20]	693	-	683	-	-
Ge2	743	792	689	674	103
Ge4	755	802	693	673	109
Ge6	769	812	706	663	106
Ge8	757	814	710	673	104

the thermal cycle stability of martensite in $Co_{64}V_{16}Si_{20-x}Ge_x$ (x=2, 4, 6, 8) alloys. Fig.6 shows ten times thermal cycling curves. Fig.7 is the variation of martensitic transformation parameters and latent heat along with the thermal cycles. The $H_{A\rightarrow M}$ is the heat in the process of martensitic transformation: the area forms by the exothermic peak in the DSC curve. The $H_{M\rightarrow A}$ is the heat in the process of reverse martensitic transformation: the area formed by the endothermic peak in the DSC curve. For the Ge2, Ge4 and Ge6 alloys, all the endothermic and exothermic peaks during DSC cycles almost remain unchanged, except for the first one. This means that the microstructure or the composition of martensite phase in the Ge2, Ge4 and Ge6 alloys change during the first cycle and it reaches a relatively balanced state in the rest of process. When the content of Ge reaches to 8 at%, the martensitic transformation parameters and latent heat have no obvious change during thermal cycling process. Additionally, there is a small endothermic peak labeled by the red arrows after reverse martensitic transformation, which results from the precipitation of R phase at high temperature. This peak gradually recedes until it disappears.

The microstructural evolution during thermal cycling of $Co_{64}V_{16}Si_{20-x}Ge_x$ (x=2, 4, 6, 8) are shown in Fig.8 (BSE images) and Fig.9 (OM images). By observing and comparing the changes of the alloys before and after thermal cycling, it can be seen that the (αCo) phase precipitates in the Ge2, Ge4 and Ge6 alloys in the first thermal cycle, resulting in the decrease of martensitic transformation parameters and latent

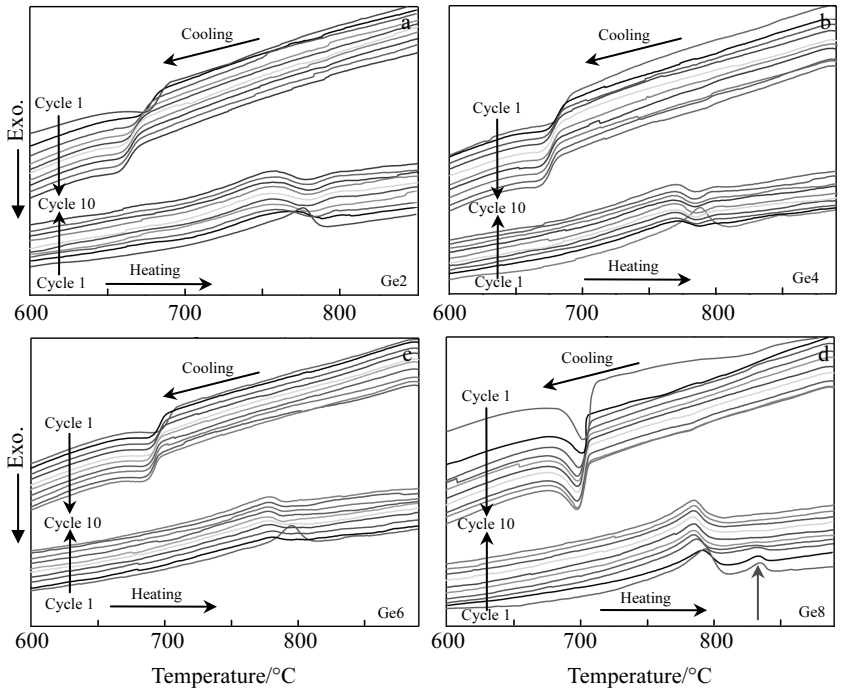

Fig.6 Ten times thermal cycling curves of the Ge2 (a), Ge4 (b), Ge6 (c) and Ge8 (d) alloys

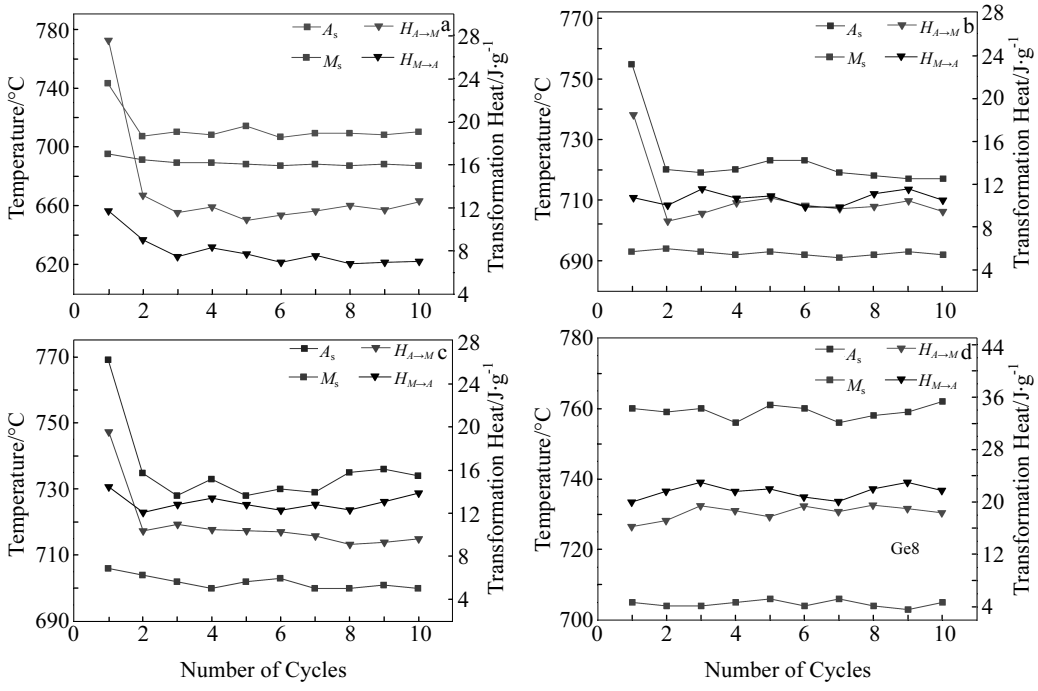

Fig.7 Transformation temperatures and latent heats in the thermal cycling curves for the Ge2 (a), Ge4 (b), Ge6 (c) and Ge8 (d) alloys

heat in the DSC curves. The precipitation of the (αCo) phase during thermal cycling process was confirmed by XRD patterns in Fig.10. During subsequent thermal cycles, the microstructure is almost unchanged. The amount of R precipitate gradually increases during thermal cycling until it reaches a balance, while the small peak in its DSC curves correspondingly recedes until it disappears, labeled by the red arrow in Fig.6. The chemical composition of each phase in the $Co_{64}V_{16}Si_{20-x}Ge_x$ (x=2, 4, 6, 8) alloys after the first and tenth thermal cycles is shown in Table 3. Comparing Table 1 and Table 3, we find that the component of each phase is relatively stable during the thermal cycle.

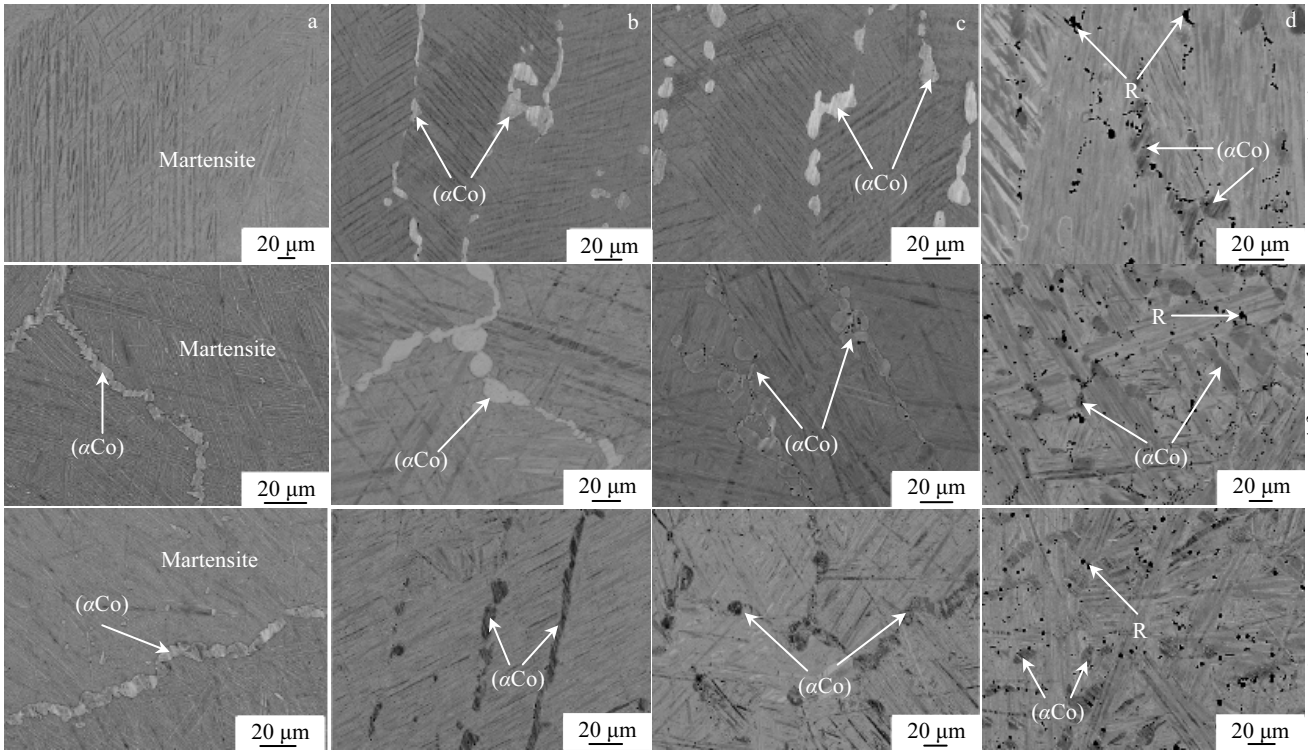

Fig.8 BSE images of Ge2 (a), Ge4 (b), Ge6 (c) and Ge8 (d) alloys during ten times thermal cycles

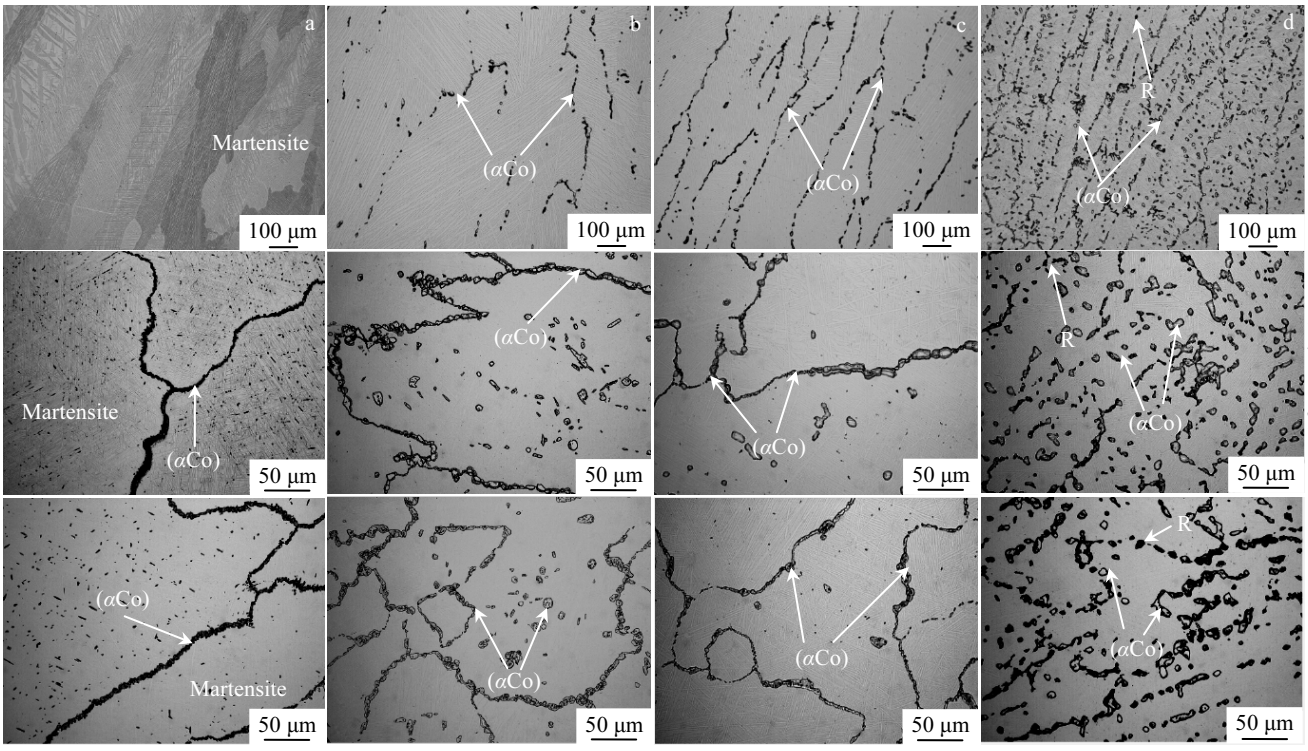

Fig.9 Optical micrographs of Ge2 (a), Ge4 (b), Ge6 (c) and Ge8 (d) alloys during ten times thermal cycles

Table 3 Chemical composition of each phase in the $Co_{64}V_{16}Si_{20-x}Ge_x$ (x=2, 4, 6, 8) alloys after the first and tenth thermal cycles (at%)

Alloy	Martensite			(αCo) phase			R phase		
	V	Si	Ge	V	Si	Ge	V	Si	Ge
Ge2-1st	17.07	17.53	1.59	11.29	9.19	1.18	-	-	-
Ge2-10th	17.13	17.75	1.58	11.18	9.12	1.09	-	-	-
Ge4-1st	16.80	15.63	3.43	13.11	8.86	2.59	-	-	-
Ge4-10th	17.14	15.99	3.65	12.27	7.79	2.69	-	-	-
Ge6-1st	16.72	13.99	5.01	13.51	7.56	3.87	-	-	-
Ge6-10th	17.04	14.38	5.22	12.14	7.09	3.61	-	-	-
Ge8-1st	16.64	12.38	7.28	14.05	6.26	5.74	47.87	14.10	2.48
Ge8-10th	17.39	11.61	7.37	14.07	6.69	4.45	48.50	12.69	2.35

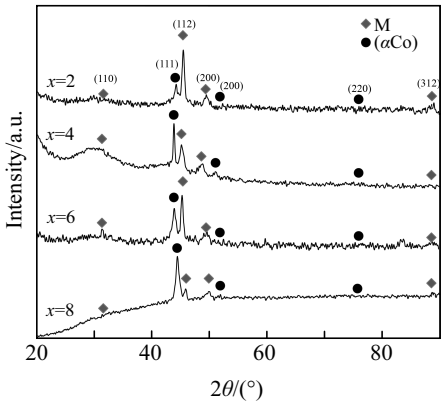

Fig.10 XRD patterns of the $Co_{64}V_{16}Si_{20-x}Ge_x$ (x=2, 4, 6, 8) alloys after the tenth thermal cycle

3 Conclusions

1) A typical lamellar single martensite is observed in the Ge2 alloy. With the increase of Ge content, the (αCo) phase precipitates from the grain boundaries. Thus the two-phase microstructure of $D0_{22}$ martensite and (αCo) phase is observed in the Ge4 and Ge6 alloys and the three-phase microstructure of $D0_{22}$ martensite, (αCo) phase and R phase is observed in the Ge8 alloy.

2) The reverse martensitic transformation temperature increases by nearly 50 °C with the addition of Ge. The reversible martensitic transformation peaks are observed during ten times thermal cycles. The alloys show a good thermal cycling stability. The thermal stability of the Co-V-Si HTSMAs can be improved by alloying Ge.

References

1 Firstov G S, Van Humbeeck J, Koval Y N. *Journal of Intelligent Material Systems and Structures*[J], 2006, 17(12): 1041

2 Jani J M, Leary M, Subic A *et al. Materials & Design*[J], 2014, 56: 1078

3 Sedmák P, Šittner P, Pilch J *et al. Acta Materialia*[J], 2015, 94: 257

4 Patriarca L, Wu Y, Sehitoglu H *et al. Scripta Materialia*[J], 2016, 115: 133

5 Saghaian S M, Karaca H E, Souri M *et al. Materials & Design*[J], 2016, 101: 340

6 Saygili H H, Tugrul H O, Kockar B. *Shape Memory and Superelasticity*[J], 2019, 5: 32

7 Xin Y, Li Y. *Materials Science and Engineering A*[J], 2016, 649: 254

8 Timofeeva E E, Panchenko E Y, Pichkaleva M V *et al. Materials Letters*[J], 2018, 228: 490

9 Yao J, Cui B, Zheng X H *et al. Vacuum*[J], 2018, 147: 78

10 Pérez-Checa A, Feuchtwanger J, Barandiaran J M *et al. Scripta Materialia*[J], 2018, 154: 131

11 Wang C P, Su Y, Yang S Y *et al. Smart Materials and Structures*[J], 2014, 23: 025 018

12 Zhang X, Liu Q S. *Intermetallics*[J], 2018, 92: 108

13 Zhang X, Wang Q, Zhao X *et al. Applied Physics A*[J], 2018, 124: 242

14 Ma J, Karaman I, Noebe R D. *International Materials Reviews*[J], 2010, 55(5): 257

15 Sahay S K, Goswami B. *Solid State Phenomena*[J], 2009, 150: 197

16 Xu X, Omori T, Nagasako M *et al. Applied Physics Letters*[J], 2013, 103: 164 104

17 Umetsu R Y, Okubo A, Xu X *et al. Journal of Alloys and Compounds*[J], 2014, 588: 153

18 Hirata K, Xu X, Omori T *et al. Journal of Alloys and Compounds*[J], 2015, 642: 200

19 Jiang H X, Wang C P, Xu W W *et al. Materials & Design*[J], 2017, 116: 300

20 Jiang H X, Xu X, Omori T *et al. Materials Science and Engineering A*[J], 2016, 676: 191

21 Xu X, Nagashima A, Nagasako M *et al. Applied Physics Letters*[J], 2017, 110: 121 906

22 Yu H J, Fu H, Sun J X *et al. Journal of Alloys and Compounds*[J], 2009, 477(1-2): 628

23 Yu H J, Fu H, Wang Z G *et al. Materials Science and Engineering A*[J], 2009, 507(1-2): 37

24 Yu H J, Jiang X D, Fu H *et al. Journal of Alloys and Compounds*[J], 2010, 490(1-2): 326

25 Han Z D, Wang D H, Zhang C L *et al. Materials Science and Engineering B*[J], 2009, 157(1-3): 40

26 Lu X, Chen X, Qiu L *et al. Journal de Physique IV (Proceedings)*[J], 2003, 112: 917
27 Xuan H C, Han P D, Wang D H *et al. Journal of Alloys and Compounds*[J], 2014, 582: 369
28 Gupta K P. *Journal of Phase Equilibria and Diffusion*[J], 2005, 26: 374

Ge 元素的添加对 Co-V-Si 高温形状记忆合金的组织和热稳定性能的影响

王翠萍[1]，黄路生[1]，张晏清[1]，张锦彬[1]，蒋恒星[1]，杨水源[1]，刘兴军[1,2,3]
(1. 厦门大学 福建省材料基因工程重点实验室，福建 厦门 361005)
(2. 哈尔滨工业大学 先进焊接与连接国家重点实验室，黑龙江 哈尔滨 150001)
(3. 哈尔滨工业大学 材料基因工程与大数据研究所，广东 深圳 518055)

摘　要：对 $Co_{64}V_{16}Si_{20}$ 形状记忆合金中的硅元素用锗元素取代进行了研究。系统研究了 $Co_{64}V_{16}Si_{20-x}Ge_x$ (x=2, 4, 6, 8, at%)系列合金在热循环过程中的组织、马氏体转变、热循环稳定性和微观结构演化。当 x=2 时，合金为具有 $D0_{22}$ 结构的单相马氏体组织。随着 Ge 含量增加到 4 at%和 6 at%，观察到(αCo)相和 $D0_{22}$ 马氏体相的两相组织。当 Ge 含量达到 8 at%时，合金呈现(αCo)相+$D0_{22}$ 马氏体相+R 相的三相组织。结果表明，与 $Co_{64}V_{16}Si_{20}$ 基体合金相比，加入锗元素进行合金化可使可逆马氏体转变温度提高近 50 ℃。虽然在热循环过程中伴随着(αCo)相或 R 相的析出，但是可逆马氏体相变峰仍然出现在 10 次热循环中。结果表明，锗元素的添加可以改善 Co-V-Si 高温形状记忆合金的热循环稳定性。

关键词：Co-V-Si-Ge；马氏体转变；热稳定性；高温形状记忆合金

作者简介：王翠萍，女，1963 年生，博士，教授，厦门大学材料学院，福建 厦门 361005，电话：0592-2180606，E-mail: wangcp@xmu.edu.cn